Nanoporous Polymers Containing Stereocontorted Cores for Hydrogen Storage

Shengwen Yuan,[†] Scott Kirklin,[‡] Brian Dorney,[‡] Di-Jia Liu,*[,‡] and Luping Yu*[,†]

Department of Chemistry and The James Franck Institute, The University of Chicago, 929 E. 57th Street, Chicago, Illinois 60637, and Chemical Sciences & Engineering Division, Argonne National Laboratory, 9700 S. Cass Ave., Argonne, Illinois 60439

Received October 24, 2008; Revised Manuscript Received January 12, 2009

ABSTRACT: This paper reports synthesis of several nanoporous polymers containing stereocontorted cores for hydrogen storage. The spirobifluorene and tetraphenylmethane cores were used as the building blocks for the cross-linked polymers. Trimerizations of acetylinic compounds or oxidative coupling of thiophenyl compound were used for the polymerization. Characterizations on structures and hydrogen storage capacities of the resulting polymers were performed. It was found that the polymers thus prepared generally have a narrow pore size distribution, and specific surface areas up to 1000 m^2/g were obtained. It was shown that the reaction conditions affect the size of nanopores and the surface areas. Hydrogen adsorption capacities at liquid nitrogen and ambient temperatures were measured using a Sievert isotherm apparatus.

Introduction

Molecular hydrogen is the cleanest energy carrier because it generates water after electro-oxidation in fuel cells. Hydrogen-based energy technology becomes increasingly important amid rapid rise of oil price and accelerated global warming from fossil fuel consumption. Among major technical barriers associated with the H_2-powered fuel cell vehicle, on-board storage of sufficient quantity of hydrogen remains the bottleneck challenge for commercialization. During the past two decades, a variety of high surface area, physisorption-based materials were investigated to store hydrogen under safe and economical conditions, including metal organic framework, carbon nanotubes, and cross-linked polymers.[1–13] Among those materials, metal organic frameworks were reported with very high adsorption capacity up to 7.5% mass of hydrogen at 70 bar and 77 K.[3]

Highly porous polymeric materials adsorb hydrogen via physisorptive mechanism and could potentially provide promising performance due to its lightweight, chemical and thermal stabilities, and structural flexibility. One particular type of such materials is termed as the polymer of intrinsic microporosity (PIM), whose porosity is independent of the processing history.[4–9] Typical surface areas of PIMs range from 300 to 1500 m^2/g. The best example to date is trip-PIM based on a triptycene monomer, which takes up 2.7% H_2 by mass at 10 bar and 77 K or 3.04% at 15 bar and 77 K. On the basis of a tentative extrapolation of H_2 sorption capacity versa the PIM surface area, it was suggested that a PIM with surface area of 2400 m^2/g could potentially adsorb more than 6% H_2 by mass at 15 bar and 77 K, though the synthetic approach to such high surface area materials remains a challenge.[4] Hyper-cross-linked polymers, prepared through Friedel−Crafts alkylation of benzyl chorides,[10–13] N-alkylation of alkyl dihalides, or polyhalogen benzenes with polyaniline or diaminobenzene,[14,15] were also reported. Surface area as high as 1904 m^2/g was obtained by Cooper and co-worker in hyper-cross-linked polymer materials prepared through self-condensation of bischloromethyl monomers, and the polymer could adsorb 3.7 % H_2 by mass at 15 bar and 77 K. Other types of synthetic approaches to prepare porous polymers including amide and imide formation as well as palladium-catalyzed Sonogashira and Suzuki coupling were recently investigated.[16–18] A crystalline organic polymer, an analogue of MOF, was prepared from tetra(4-dihydroxyborylphenyl)methane with reported BET surface area as high as 4210 m^2/g based on argon adsorption isotherm.[19] However, all of the reported materials have yet to demonstrate high hydrogen storage capacity at ambient temperature which is critical for the transportation application.[20] In addition to the higher surface area, a crucial attribute for the adsorbent is the heat of adsorption that should be sufficiently high to retain hydrogen at room temperature yet low enough to release the hydrogen when it is needed without raising the storage bed temperature significantly.

Reported here is the first group of a series of porous polymers investigated in our laboratories for the hydrogen storage application. We started from the hypothesis that polymers with high surface area and narrow pore distribution with delocalized π-electron systems may interact attractively with hydrogen molecules through enhanced van der Waals interaction. Furthermore, introducing heteroatomic functional groups that modify the electron conductivity of the polymer backbone may also improve the dipole−induced dipole interaction between hydrogen and adsorbent. We therefore designed and synthesized a series of cross-linked polymers containing spirobifluorene and tetraphenylmethane as the contortive cores via trimerization of the terminal acetylene groups or oxidative coupling of the terminal thiophenes. Several of these polymers are cross-linked, fully conjugated systems. Polymers with surface areas exceeding 1000 m^2/g were obtained, and hydrogen sorption capacity reached 2.2 wt % at 77 K and 7 bar and 0.43 wt % at 298 K and 70 bar. In this paper, we report results on synthesis, structural characterization, and hydrogen uptake capacity measurements of four such polymers, which shed light on future directions for the research in these types of polymers.

Results and Discussion

Synthesis of Monomers and Porous Polymers. As outlined in Schemes 1−3, two types of monomers with spiral and tetrahedral core structures were selected for constructing intrinsic porosity within the polymers. The spirobifluorene and tetraphenylmethane cores were synthesized according to modified literature procedures.[21,22] These hydrocarbons were further converted into tetrabromo compounds. The palladium-mediated

* Corresponding authors. E-mail: lupingyu@midway.uchicago.edu and djliu@anl.gov.
[†] The University of Chicago.
[‡] Argonne National Laboratory.

10.1021/ma802394x CCC: $40.75
Published on Web 02/13/2009

Scheme 1. Synthesis of Polymer PS4AC1/PS4AC2

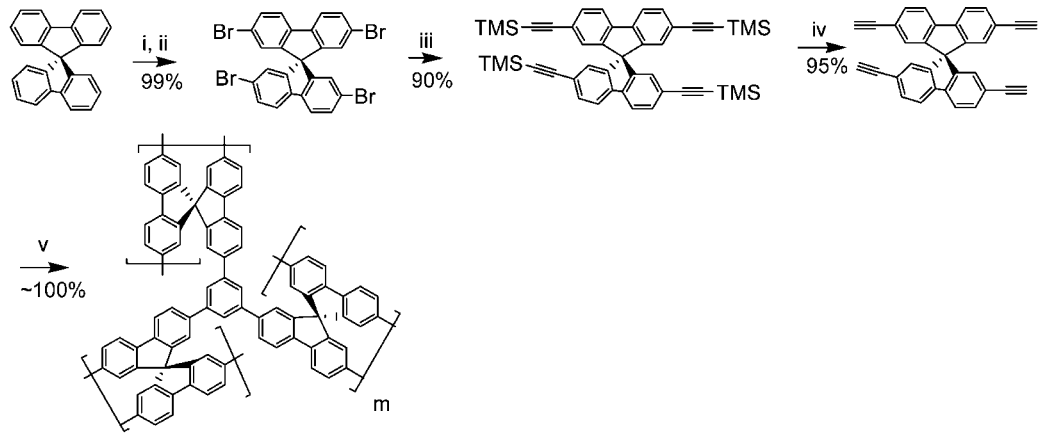

PS4AC1/PS4AC2

i) $CHCl_3$, Fe powder (6%mol); ii) Br_2 (neat, 4.3eq) was added at 0°C, then warm to RT 3-5h; iii) i-Pr_2NH, (Trimethylsilyl)acetylene (4.8eq), $PdCl_2(PPh_3)$ (8%mol), CuI (4%mol), PPh_3(16%mol), reflux for 12h; iv) CH_2Cl_2, NaOH (10eq) in CH_3OH, RT, 6h; v) Dioxane (dry), $Co_2(CO)_8$ (0.24 eq for **PS4AC1,** 2/3 eq for **PS4AC2**) , 110°C. 1h.

Scheme 2. Synthesis of Polymer PT4AC

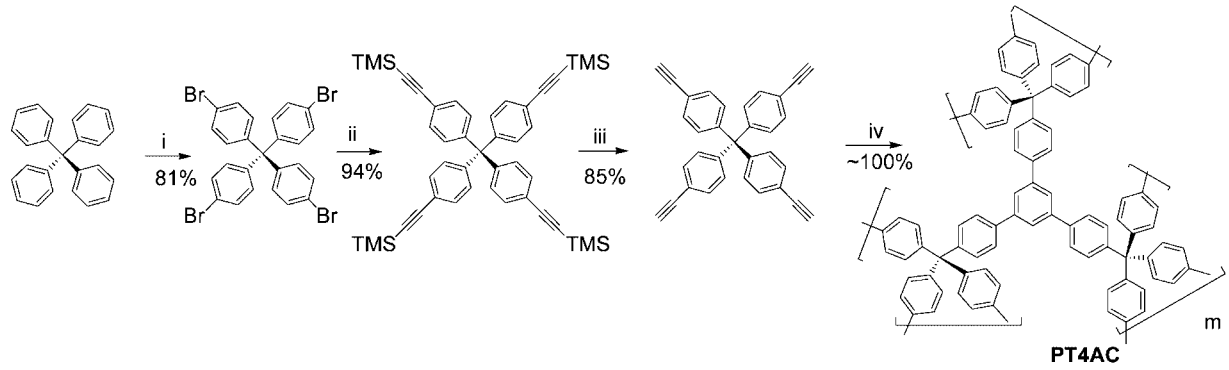

PT4AC

i) Br_2 (neat, 7eq) was added during 5 min period, RT, vigorous stir for 30min; ii) i-Pr_2NH/THF(1:3), (Trimethylsilyl)acetylene (4.8eq), $PdCl_2(PPh_3)$ (8%mol), CuI (4%mol), PPh_3(16%mol), reflux for 24h; iii) CH_2Cl_2, NaOH (10eq) in CH_3OH, RT, 6h; iv) Dioxane (dry), $Co_2(CO)_8$ (24%mol), 110°C, 1h.

Scheme 3. Synthesis of Polymer PS4TH

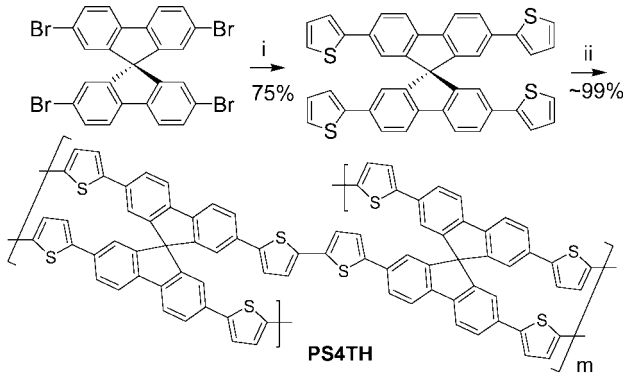

PS4TH

i) 2-tributyltinthiophene (8eq), $Pd(PPh_3)_4$ (6%mol), dry THF, reflux 24h; ii) $FeCl_3$ (8eq), dry $CHCl_3$, RT, 24h;

Sonagashira and Stille coupling reactions were used to introduce the acetylenyl and thiophenyl units, respectively. The monomers containing terminal acetylene groups were subject to trimerization catalyzed by cobalt carbonyl complex, which led to cross-linked polymers **PS4AC1**, **PS4AC2**, and **PT4AC**.[23] The monomer containing thiophene attached to the 2,2′,7,7′-positions of spirobifluorene was polymerized through oxidative coupling to form porous polymers **PS4TH**, which exhibit extended conjugation systems.

Structural Characterizations. The resulting polymers are all heavily cross-linked and insoluble in any solvent, which limited our means to perform structural characterization. However, FTIR spectrometers offer assistance in deciphering the structural information. The degree of trimerization of the terminal acetylene groups was determined by comparing the FTIR spectra of the polymers and respective monomers. Relative peak intensity of the C−H stretching from C≡C−H (around 3300 cm^{-1}) and C−H bending from Ar−H (around 820 cm^{-1}) of the monomers and polymers were calculated using the absorbance ratio $R = A(3300\ cm^{-1})/A(820\ cm^{-1})$, where A is the absorbance peak height at the specified frequency. The values obtained are $R_{MS4AC} = 1.33$, $R_{PS4AC1} = 0.25$, $R_{PS4AC2} = 0$, $R_{MT4AC} = 0.63$, and $R_{PT4AC} = 0.25$ (**MS4AC**, and **MT4AC** are the two monomers corresponding to the synthesis of polymers **PS4AC1** and **PT4AC**, respectively). Since the bending vibration intensity of C−H from Ar−H will not be affected much by the polymerization, the decrease in the value of this ratio indicated the degree of the cross-linking. The polymerization shown by IR spectra, however, is not complete except

Table 1. Surface Properties and Hydrogen Uptake Capacities of Selected Polymers

	BET surface area (m^2/g)	Langmuir surface area (m^2/g)	micropore surface area (m^2/g)	total pore volume (cm^3/g)	micropore volume (cm^3/g)	H−K median pore diameter (nm)	H_2 gravimetric uptake (%) at 77 K (kg H_2/ kg adsorbent + H_2(ads))[a]	H_2 gravimetric uptake (%) at 298 K (kg H_2/ kg adsorbent + H_2(ads))[b]
PS4AC1	769	1122	492	0.427	0.249	0.62	2.8	0.44
PT4AC	762	1114	448	0.425	0.226	0.64	2.2	0.50
PS4AC2	1043	1412	496	0.477	0.251	0.67	3.7	0.43
PS4TH	971	1439	443	0.757	0.223	0.62	3.6	0.45

[a] Hydrogen uptake capacities at 77 K were measured at H_2 equilibrium pressure of 60 bar. [b] Hydrogen uptake capacities at 298 K were measured at H_2 equilibrium pressure of 70 bar.

for **PS4AC2**. This result is consistent with our controlled reaction condition. The trimerization reaction proceeds very quickly, and the polymers precipitated out within minutes before the cobalt catalyst can diffuse into the reaction mixture. These factors led to low cross-linking density and low porosity in polymer **PS4AC1** and **PT4AC**. When the catalyst ratio of Co over the triple bonds was increased to 1/3 while keeping other conditions unchanged, polymer **PS4AC2** was obtained with almost completed conversion of the terminal acetylene units. Consequently, an enhanced surface area was achieved (Table 1).

Representative FTIR spectra of a polymer and its corresponding monomer are shown in Figure 1. Carbon−hydrogen stretching peak from C≡C−H was still distinct in **PS4AC1** and **PT4AC** samples, but almost not detectable in **PS4AC2.** We reasoned that larger amount of catalyst created more reaction sites for **PS4AC2.** A new absorption peak at 795 cm^{-1} was observed from the FTIR spectrum of **PS4TH** comparing with the FTIR spectrum of **MS4TH** (the corresponding monomer of **PS4TH**), which is the characteristic peak of 2,5-disubstituted thiophenes (Figure 1c).[24] These results provide the evidence for the homocoupling of the terminal thiophene units.

The thermal properties of these polymers were characterized by thermal gravimetric analysis (TGA) and differential scanning calorimetry (DSC). Figure 2 shows the TGA graphs for polymers **PS4AC1**, **PS4AC2**, **PT4AC**, and **PS4TH**. It was found that most of these polymers were stable up to the temperature range of 300−380 °C after an initial weight loss of 5%−15%, which may be due to loss of the trapped solvent, moisture, or catalyst residue. No distinct glass transition for these polymers was observed due to the nature of their cross-linked structures.

Porous Polymer Surface Properties. The surface properties of the polymers were studied by the nitrogen BET method using a Micromeritics ASAP 2010 system. Some representative nitrogen adsorption/desorption isotherms of these polymers are shown in Figure 3. Polymers **PS4AC1, PS4AC2**, and **PT4AC** exhibit type IB isotherms, whereas **PS4TH**'s isotherms have type II characteristics. Listed in Table 1 are the key structural properties derived from the isotherm data such as BET and Langmuir surface areas, micropore surface areas and volumes, total pore volume, and median pore diameters based on slit-pore model of the Horvath−Kawazoe (H−K) method. While the BET or Langmuir surface areas vary significantly, it is interesting to note that the values of microporous volume and surface area are rather consistent among these samples, presumably due to the fact that similar molar fraction of contorted linkers were used in the polymer synthesis which control the formation of micropores. Shown in Figure 4 is the incremental surface area as the function of the pore width for polymer **PS4TH**, which was calculated from the density function theory (DFT). A particularly important observation is that the polymers have relatively narrow pore size distribution with a majority of pores having the width ranging from 0.6 to 0.8 nm. It is worth noting that the median pore widths of all the polymers we prepared are all in the range of 0.6−0.7 nm based on the H−K model, which is consistent with the observation of other porous polymers and has been suggested to be desirable for better interaction between hydrogen molecules and the pore walls.[10] Narrow pore distribution appears to be an unique advantage of porous polymer adsorbents, in addition to the flexibility of

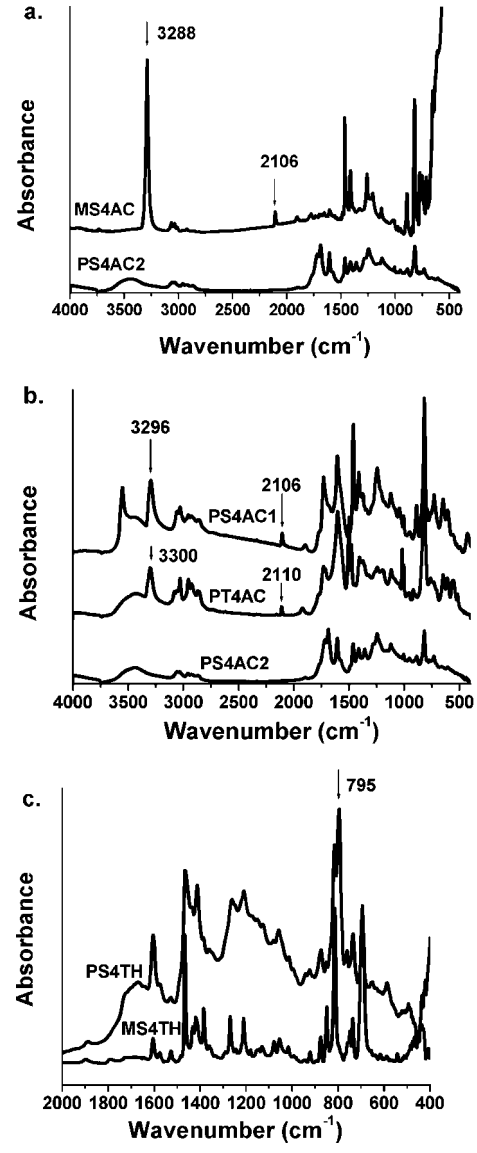

Figure 1. (a) FTIR of polymer **PS4AC2** and its corresponding monomer **MS4AC**; peak intensity at 3288 and 2106 cm^{-1} decreases dramatically, indicating consumption of acetylene functional groups during the polymerization reaction. (b) FTIR of polymers **PS4AC1**, **PS4AC2**, and **PT4AC**; alkynyl carbon−hydrogen bond vibration band around 3300 cm^{-1} and C≡C triple bond vibration band around 2110 cm^{-1} are still distinct in polymer **PS4AC1** and **PT4AC**, but almost completely diminished in **PS4AC2**. (c) FTIR of tetrathiophene spirobifluorene monomer **MS4TH** and its corresponding polymer **PS4TH**.

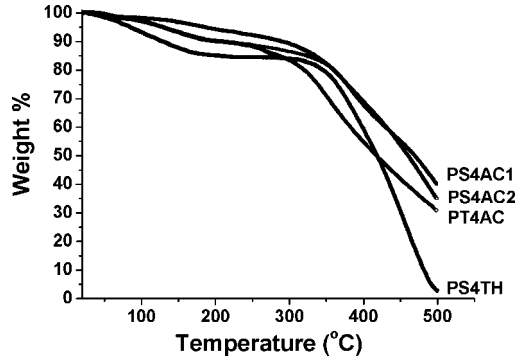

Figure 2. TGA graph of polymers **PS4AC1**, **PS4AC2**, **PT4AC**, and **PS4TH**.

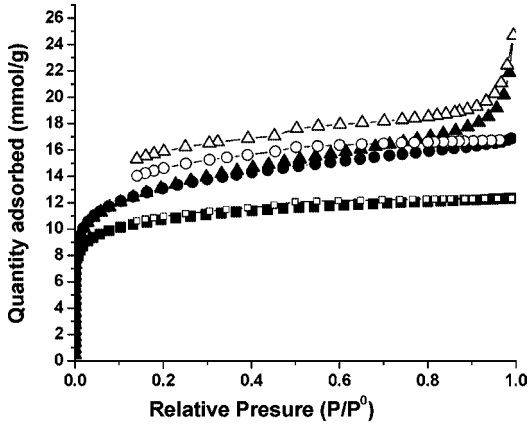

Figure 3. Nitrogen adsorption isotherm (filled symbols) and desorption isotherm (open symbols) at 77 K for polymers **PS4AC1** (square symbol), **PS4AC2** (circle symbol), and **PS4TH** (triangle symbol). The isotherms of **PT4AC** mostly overlap with those of **PS4AC1** and are not shown here for clarity purposes.

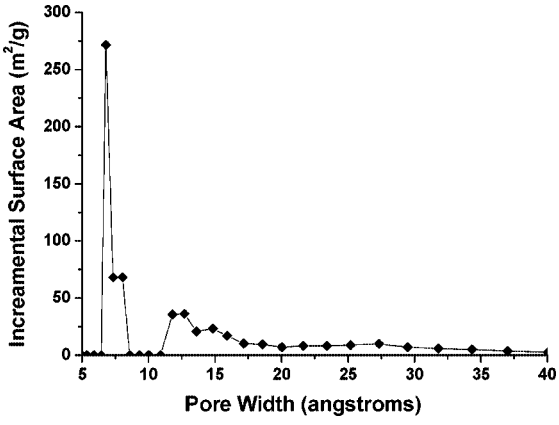

Figure 4. DFT analysis on incremental area vs pore width for **PS4TH**.

introducing noncarbon elements and different functional groups through the synthesis approach.

Hydrogen Sorption Capacities. The excess hydrogen adsorption capacities of polymers were measured by a Sievert type isotherm apparatus with similar design and analysis method as that reported in the literature.[25] To ensure the accuracy of the measurement, we prepared and measured a well-documented metal organic framework (MOF) sample, Cu-BTC (BTC: benzene-1,3,5-tricarboxylate),[3,26,27] using our apparatus and obtained essentially the identical results as previously reported (see Supporting Information). Shown in Figure 5 is a representative example of the adsorption/desoprtion isotherms for the

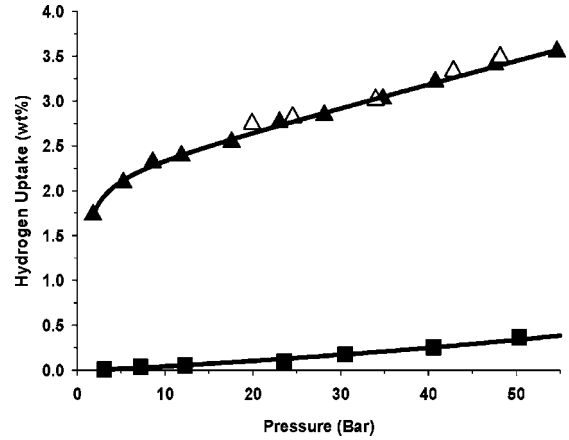

Figure 5. Gravimetric hydrogen adsorption isotherms (solid symbol) and desorption isotherm (open symbol) for polymers **PS4TH** at liquid nitrogen temperature (triangle symbol) and ambient temperature (square symbol).

polymers we investigated. In this case, the gravimetric hydrogen uptake by **PS4TH** was measured at both liquid nitrogen and ambient temperatures. A type II isotherm at 77 K and near linear uptake at room temperature as the function of adsorption pressure is characteristic for all the polymers of this study. Complete overlap between adsorption and desorption curves suggests no hysteresis between the two processes. We also investigated adsorption/desorption in multiple cycles and found the isotherm plots essentially repeat with each other within the measurement error. Listed in Table 1 are the average hydrogen adsorption capacities of all the polymers measured at both temperatures. The adsorption capacity as high as 3.6 wt % was obtained for **PS4TH** at liquid nitrogen temperature and 60 bar. At lower pressure of 7 bar and 77 K, the adsorption capacities for **PS4AC1**, **PT4AC**, **PS4AC2**, and **PS4TH** are 1.7, 1.2, 2.2, and 2.1 wt %, respectively. The adsorption capacity is generally proportional to the BET surface area at 77 K, following the so-called "Chahine rule" despite the differences in the polymer molecular structures. This is relatively easily understood since, at 77 K, the kinetic energy of hydrogen molecule succumb to the heat of adsorption at the polymer surface and H_2 will adsorb and populate any available surface. Another observation is that we did not reach the adsorption saturation for these polymers with the pressure up to 60 bar, which is different from the case of MOF Cu-BTC (see Supporting Information). The root cause of which is currently under continuous investigation.

At room temperature, we found that the hydrogen adsorption in these polymers was moderate, nonetheless significant, ranging from 0.43 to 0.5 wt % at 70 bar. The differences in adsorption capacity become less significant among the polymer samples. Dissimilar molecular structures do not seem generate substantial differences in adsorption capacity. For example, one would expect somewhat higher capacity for **PS4TH** in comparison with **PS4AC2** if indeed there is an enhanced interaction between the hydrogen and the conductive functional group of thiophene. The fact that very close hydrogen adsorption capacities are observed between the two at ambient temperature suggests that enhancement may not have significant impact. The preliminary result from ab initio calculation indicated that such interaction is indeed relatively weak.[28] From our observation, nonetheless, we do speculate that adsorption capacity at ambient temperature may be more sensitive to the microporosity since all the polymers in this study have similar micropore surface areas and diameters. To experimentally prove this, however, requires the preparation of polymers with significantly different microporous properties.

Conclusion

Several nanoporous polymers containing stereocontorted cores were synthesized as materials for hydrogen storage. Surface areas up to 1000 m^2/g with desirable narrow pore distributions were obtained. It was found that hydrogen adsorption capacity at liquid nitrogen temperature is generally proportional to the surface area. The extended π-electron system and introduction of sulfur heteroatom did not seem to significantly affect the adsorption of hydrogen although more detailed modeling and thermodynamic studies on H_2−adsorbent interaction is underway. The results indicate that, to significantly increase the heat of adsorptions thus adsorption capacities at ambient temperature, new functional groups with strong interactions with hydrogen molecules are needed. The versatility of polymer design and synthesis offers vast opportunities in the adsorbent composition and structural improvements which will be actively pursued.

Experimental Section

Materials. Chemicals were purchased from Aldrich, Alfa Asia, and Strem and were used without further purification unless otherwise noted. Tetrahydrofuran (THF) anhydrous solvent was distilled from commercial THF with sodium/benzophenone ketyl. Dioxane and *i*-Pr_2NH anhydrous solvents were distilled from their respective mixture with CaH_2.

Equipment. ^1H and ^{13}C NMR spectra were collected on a Bruker 400 or 500 MHz FT NMR spectrometer. FTIR spectra were recorded on a Thermo Nicolet Nexus 670 FTIR spectrometer. Elemental analyses were performed by Atlantic Microlab, Inc., and Columbia Analytical Services, Inc. TGA data were obtained from a Shimadzu TGA-50 with a heating rate of 10 °C/min in ambient air. DSC data were obtained from a Shimadzu DSC-60 with a heating rate of 10 °C/min in a nitrogen atmosphere. Nitrogen BET surface area and porosity were measured using a Micromeritics ASAP 2010 system.

The hydrogen adsorption isotherms at 77 K and ambient temperature were measured with a modified Sievert isotherm apparatus similar to that reported in the literature.[25] In our study, typical polymer sample sizes ranged from 200 to 500 mg. Before each isotherm measurement, the sample was heated at 125 °C under vacuum to remove residual moisture or other trapped gases. Ultrahigh purity helium (99.9995%) was used to calibrate the free volume in the sample cell before each measurement. For H_2 update measurement, hydrogen with purity of 99.9995% was used. The ambient temperature was controlled through an isolated hood, and 77 K measurement was conducted by immersing the sample cell into liquid nitrogen dewar. Hydrogen equilibrium pressure as high as 70 bar was applied for the measurement. A typical measurement error was $<\pm 10\%$ of the full hydrogen uptake capacity at high-pressure limit. The error reduced to $<\pm 5\%$ at the low-pressure region. A commercial software, GASPAK, was used to accurately calculate the state equations of the hydrogen and helium under different pressures and temperatures.

Synthesis of 2,2′,7,7′-Tetrabromo-9,9′-spirobifluorene. Fe powder (0.075 g, 1.33 mmol) was added to a solution of 9,9′-spirobifluorene (7.0 g, 22.1 mmol) in 33 mL of chloroform, the mixture was then cooled to 0 °C, and then neat bromine (4.9 mL, 95.03 mmol) was added slowly via a syringe. The mixture was stirred at 0 °C for 1 h, then warmed to room temperature, and continued stirring for another 3−5 h, and the evolved HBr gas was exported to a NaOH solution. The reaction mixture was then poured into saturated Na_2CO_3 solution to remove the excess Br_2 and extracted with CH_2Cl_2 twice. The combined organic phase was washed with brine once, separated, and dried over anhydrous Na_2SO_4. After removing the solvent, white solid product (14.0 g, 99% yield) was obtained in its pure form. Further purification could be done by crystallization from the $CHCl_3$/EtOH mixture. ^1H NMR: δ (ppm): 6.82 (d, $J = 1.6$ Hz, 4H, Ar−H), 7.54 (dd, $J = 1.8$, 8.2 Hz, 4H, Ar−H), 7.68 (d, $J = 8.2$ Hz, 4H, Ar−H), which is consistent with reported result.[16]

Synthesis of 2,2′,7,7′-Tetra(2-(trimethylsilyl)ethynyl)-9,9′-spirobifluorene. 2,2′,7,7′-Tetrabromo-9,9′-spirobifluorene (3.0 g, 4.75 mmol), $PdCl_2(PPh_3)_2$ (0.26 g, 0.37 mmol), CuI (0.036 g, 0.19 mmol), and PPh_3 (0.2 g, 0.76 mmol) were placed in a round-bottom flask; anhydrous *i*-Pr_2NH (50 mL) and trimethylsilylacetylene (3.24 mL, 22.8 mmol) were added via a syringe. The reaction mixture was brought to reflux overnight and then cooled down to room temperature. Solvent was removed in vacuum, and $CHCl_3$ was added to dissolve the residue and filtered through a pad of Celite. The filtrate was washed with dilute Na_2EDTA solution and then dried over anhydrous Na_2SO_4; the solution was concentrated, and ethanol was added to obtain white solid product (3.0 g, 90% yield) in its pure form. ^1H NMR: δ (ppm): 0.16 (s, 36H, CH_3), 6.77 (d, $J = 0.8$ Hz, 4H, Ar−H), 7.49 (dd, $J = 1.4$, 7.9 Hz, 4H, Ar−H), 7.74(d, $J = 7.9$ Hz, 4H, Ar−H). ^{13}C NMR: δ (ppm): 0.4, 96.1, 106.0, 121.4, 124.0, 128.9, 133.4, 142.5, 149.2.

Synthesis of 2,2′,7,7′-Tetraethynyl-9,9′-spirobifluorene. NaOH (0.286 g, 7.1 mmol) was dissolved in 5 mL of CH_3OH, then added to a solution of 2,2′,7,7′-tetra(trimethylsilylacetyl)-9,9′-spirobifluorene (0.5 g, 0.71 mmol) in 20 mL of CH_2Cl_2, and then stirred for 6 h at room temperature. The reaction mixture was washed with water, and the aqueous phase was extracted with CH_2Cl_2 once the combined organic phases were washed with brine, and then dried over anhydrous Na_2SO_4. The solution was concentrated, and ethanol was added to the solution. Light yellow solid product (0.273 g, 95% yield) was obtained in its pure form. ^1H NMR: δ (ppm): 3.01 (s, 4H, C≡CH), 6.866 (d, $J = 0.8$ Hz, 4H, Ar−H), 7.54 (dd, $J = 1.4$, 7.9 Hz, 4H, Ar−H), 7.80(d, $J = 7.9$ Hz, 4H, Ar−H).

Synthesis of Polymer PS4AC1. 2,2′,7,7′-Tetraethynyl-9,9′-spirobifluorene (0.849 g, 2.06 mmol) was charged into a flame-dried round-bottom flask; anhydrous dioxane (17 mL) was added via a syringe and stirred to get a clear light yellow solution. $Co_2(CO)_8$ (0.169 g, 0.494 mmol) was added under protection of N_2, kept stirring for a while, and then placed the flask into an oil bath that was preheated to 115 °C. The brown solution started to solidify after about 5 min. The reaction mixture was continued heating for another 5 min, and then the flask was lifted above the oil bath to cool to room temperature. The brown solid was smashed to fine particles using a spatula, then washed with methanol, and filtered to collect the solid. After air-drying for an hour, the solid was dried in vacuum oven at 90 °C for 2 days. About 1.0 g (∼100% yield) of brown solid was obtained. Elemental Analysis: Calculated for $[C_{33}H_{16}]_x$: C, 96.09; H, 3.91. Found: C, 74.12; H, 3.94; Co, 3.63; corresponding to formula $\{C_{33}H_{16}(H_2O)_4[Co_2(CO)_8]_{0.16}\}_x$, which suggests the polymer contains 4 H_2O and 0.16 $Co_2(CO)_8$ per repeating unit. To verify potential impact of residual cobalt complex, another sample **PS4AC** was obtained by washing away the cobalt catalyst from **PS4AC1**: right after air-drying, polymer **PS4AC1** was grinded into powder and stirred into 40 mL of 37% HCl solution for 2 h at room temperature. The resulting mixture was filtered, washed with water and methanol, and then dried in vacuum oven at 90 °C for 2 days. Elemental Analysis: Calculated for $[C_{33}H_{16}]_x$: C, 96.09; H, 3.91. Found: C, 85.04; H, 4.28; Co, 0.14; corresponding to formula $\{C_{33}H_{16}(H_2O)_2O[Co_2(CO)_8]_{0.006}\}_x$, which suggests the polymer contains 2 H_2O and 0.006 $Co_2(CO)_8$ (and probably 0.5 oxygen molecule from air) per repeating unit. **PS4AC** has a similar BET surface area to that of **PS4AC1** as expected. Hydrogen adsorption capacities of **PS4AC** at room temperature and 77 K were also very close to those of **PS4AC1**, suggesting little impact to the adsorption capacity by the residual Co complex in our samples.

Synthesis of Polymer PS4AC2. 2,2′,7,7′-Tetraethynyl-9,9′-spirobifluorene (0.611 g, 1.48 mmol) was charged into a flame-dried round-bottom flask; anhydrous dioxane (15 mL) was added via a syringe and stirred to get a clear light yellow solution. $Co_2(CO)_8$ (0.338 g, 0.988 mmol) was added under protection of N_2, kept stirring for a while, and then the flask was place into an oil bath that was preheated to 115 °C. The brown solution started to solidify after about 5 min. The reaction mixture was continued heating for another 55 min, then the flask was lifted above the oil bath to cool to room temperature. The brown solid was smashed

to fine particles using a spatula, then washed with methanol, and filtered to collect the solid. After air-drying for an hour, the solid was stirred into 40 mL of 37% HCl solution for 2 h at room temperature. The resulted mixture was filtered, washed with water and methanol, and dried in vacuum oven at 90 °C for 2 days. About 0.65 g (∼100% yield, containing some catalyst) of brown solid was obtained. Elemental Analysis: Calculated for $[C_{33}H_{16}]_x$: C, 96.09; H, 3.91. Found: C, 79.33; H, 3.64; Co, 0.07; corresponding to formula $\{C_{33}H_{16}(H_2O)_2O_3[Co_2(CO)_8]_{0.003}\}_x$, which suggests the polymer contains 1 H_2O, 0.003 $Co_2(CO)_8$ (and probably 1.5 oxygen molecules adsorbed from the air) per repeating unit.

Synthesis of Tetra(4-(2-(trimethylsilyl)ethynyl)phenyl)methane. Tetra(4-bromophenyl)methane (4.02 g, 6.33 mmol), $PdCl_2(PPh_3)_2$ (0.266 g, 0.37 mmol), CuI (0.048 g, 0.25 mmol), and PPh_3 (0.2 g, 0.76 mmol) were placed in a round-bottom flask; anhydrous *i*-Pr_2NH (50 mL) or a mixture of anhydrous *i*-Pr_2NH/THF (15 mL/45 mL) and trimethylsilylacetylene (4.3 mL, 30.36 mmol) was added via a syringe. The reaction mixture was brought to reflux for 24 h and then cooled down to room temperature. Solvent was removed in vacuum, and $CHCl_3$ was added to dissolve the residue and filtered through a pad of Celite. The filtrate was washed with dilute Na_2EDTA solution and then dried over anhydrous Na_2SO_4; the solution was concentrated, and ethanol was added to obtain a white solid product (4.2 g, 94% yield) in its pure form. ^{1}H NMR: δ (ppm): 0.23 (s, 36H, CH_3), 7.04 (d, J = 8.5 Hz, 8H, Ar−H), 7.33 (d, J = 8.5 Hz, 8H, Ar−H).

Synthesis of Tetra(4-ethynylphenyl)methane. The procedure for the synthesis of 2,2′,7,7′-tetraethynyl-9,9′-spirobifluorene was followed. A light yellow product was obtained in 85% yield. ^{1}H NMR: δ (ppm): 3.06 (s, 4H, C≡CH), 7.12 (d, J = 8.6 Hz, 8H, Ar−H), 7.39(d, J = 8.6 Hz, 8H, Ar−H).

Synthesis of Polymer PT4AC. The procedure for the synthesis of polymer **PS4AC** was followed. A brown solid was obtained in about 100%. Elemental Analysis: Calculated for $[C_{33}H_{20}]_x$: C, 95.16; H, 4.84. Found: C, 81.81; H, 5.40; Co, 0.15; corresponding to formula $\{C_{33}H_{20}(H_2O)_{3.75}[Co_2(CO)_8]_{0.006}\}_x$, which suggests the polymer contains 3.75 H_2O and 0.006 $Co_2(CO)_8$ per repeating unit.

2,2′,7,7′-Tetrakis(2-thienyl)-9,9′-spirobifluoene. 2,2′,7,7′-Tetrabromo-9,9′-spirobifluorene (1.99 g, 3.15 mmol), 2-(tributylstannyl)thiophene (9.4 g, 25.19 mmol), and $Pd(PPh_3)_4$ (0.146 g, 0.126 mmol) were added to a flame-dried two-neck flask under nitrogen protection. 60 mL of anhydrous THF was then added and degassed by bubbling nitrogen gas for 15 min. The reaction mixture was refluxed for 24 h and then cooled down to room temperature. THF solvent was removed and the brown-yellow solid was purified by flash chromatography on silica gel column using hexane:CH_2Cl_2 (1:1) as eluent. The fluorescent band was collected and concentrated to yield brown-yellow solid; recrystallization from $CHCl_3$/EtOH give 1.79 g of pure product (88.1% yield). ^{1}H NMR: δ (ppm): 6.95 (dd, J = 5.0 Hz, 3.7 Hz, 4H, Th−H), 6.99 (d, J = 1.5 Hz, 4H, Ar−H), 7.15 (m, 8H, Th−H), 7.66 (dd, J = 8.0 Hz, 1.6 Hz, 4H, Ar−H), 7.87 (d, J = 8.0 Hz, 4H, Ar−H).

Synthesis of Polymer PS4TH. 2,2′,7,7′-Tetrakis(2-thienyl)-9,9′-spirobifluoene (0.645 g, 1.0 mmol) was dissolved in 50 mL of anhydrous $CHCl_3$ and then transferred dropwise to a suspension of $FeCl_3$ (1.3 g, 8.0 mmol) in 15 mL of anhydrous $CHCl_3$; the resulting mixture was stirred at room temperature overnight. 200 mL of MeOH was then added to the above reaction mixture and kept stirring for another hour. The precipitation was collected by filtration and washed with MeOH and allowed to dry in air. The light brown solid was stirred into 37% HCl solution for 2 h, the suspension was then filtered and washed with H_2O and MeOH. After extracting with CH_2Cl_2 in a Soxhlet extractor for 24 h, the product was dried in vacuum oven at 100 °C overnight. Yield was about 99%. Elemental Analysis: Calculated for $[C_{41}H_{20}S_4]_x$: C, 76.84; H, 3.15. Found: C, 74.50; H, 3.43; corresponding to formula $[C_{41}H_{20}S_4(H_2O)]_x$, which confirmed that $FeCl_3$ was completely removed.

Acknowledgment. This work was supported by the U.S. Department of Energy's Hydrogen, Fuel Cells and Infrastructure Technologies program under the Office of Energy Efficiency and Renewable Energy. The authors thank Drs. Shengqian Ma and Junbing Yang for their experimental support and helpful discussions.

Supporting Information Available: Text giving nitrogen and hydrogen adsorption isotherms for a MOF Cu-BTC measured with our modified Sievert apparatus. This material is available free of charge via the Internet at http://pubs.acs.org.

References and Notes

(1) Dillon, A. C.; Jones, K. M.; Bekkedahl, T. A.; Kiang, C. H.; Bethune, D. S.; Heben, M. J. *Nature (London)* **1997**, *386*, 377–379.
(2) Rosi, N. L.; Eckert, J.; Eddaoudi, M.; Vodak, D. T.; Kim, J.; O'Keeffe, M.; Yaghi, O. M. *Science* **2003**, *300*, 1127–1130.
(3) Wong-Foy, A. G.; Matzger, A. J.; Yaghi, O. M. *J. Am. Chem. Soc.* **2006**, *128*, 3494–3495.
(4) Budd, P. M.; Bulter, A.; Selbie, J.; Mahmood, K.; McKeown, N. B.; Ghanem, B.; Msayib, K.; Book, D.; Walton, A. *Phys. Chem. Chem. Phys.* **2007**, *9*, 1802–1808.
(5) McKeown, N. B.; Budd, P. M. *Chem. Soc. Rev.* **2006**, *35*, 675–683.
(6) McKeown, N. B.; Ghanem, B.; Msayib, K. J.; Budd, P. M.; Tattershall, C. E.; Mahmood, K.; Tan, S.; Book, D.; Langmi, H.; Walton, A. *Angew. Chem., Int. Ed.* **2006**, *45*, 1804–1807.
(7) Budd, P. M.; Elabas, E. S.; Ghanem, B. S.; Makhseed, S.; Mckeown, N. B.; Msayib, K. J.; Tattershall, C. E.; Wang, D. *Adv. Mater.* **2004**, *16*, 456–459.
(8) Budd, P. M.; Ghanem, B. S.; Makhseed, S.; Mckeown, N. B.; Msayib, K. J.; Tattershall, C. E. *Chem. Commun.* **2004**, 230–231.
(9) Ghanem, B. S.; Msayib, K. J.; McKeown, N. B.; Harris, K. D. M.; Pan, Z.; Budd, P. M.; et al. *Chem. Commun.* **2007**, 67–69.
(10) Wood, C. D.; Tan, B.; Trewin, A.; Niu, H.; Bradshaw, D.; Rosseinsky, M. J.; Khimyak, Y. Z.; Campbell, N. L.; Kirk, R.; Stockel, E.; Cooper, A. I. *Chem. Mater.* **2007**, *19*, 2034–2048.
(11) Lee, J.-Y.; Wood, C. D.; Bradshaw, D.; Rosseinsky, M. J.; Cooper, A. I. *Chem. Commun.* **2006**, 2670–2672.
(12) Ahn, J.-H.; Jang, J.-E.; Oh, C.-G.; Ihm, S.-K.; Cortez, J.; Sherrington, D. C. *Macromolecules* **2006**, *39*, 627–632.
(13) Germain, J.; Hradil, J.; Frechet, J. M. J.; Svec, F. *Chem. Mater.* **2006**, *18*, 4430–4435.
(14) Germain, J.; Svec, F.; Frechet, J. M. J. *Chem. Mater.* **2008**, *20*, 7069–7076.
(15) Germain, J.; Frechet, J. M. J.; Svec, F. *J. Mater. Chem.* **2007**, *17*, 4989–4997.
(16) Weber, J.; Antonietti, M.; Thomas, A. *Macromolecules* **2008**, *41*, 2880–2885.
(17) Weber, J.; Thomas, A. *J. Am. Chem. Soc.* **2008**, *130*, 6334–6335.
(18) Jiang, J.-X.; Su, F.; Trewin, A.; Wood, C. D.; Niu, H.; Jones, J. T. A.; Khimyak, Y. Z.; Cooper, A. I. *J. Am. Chem. Soc.* **2008**, *130*, 7710–7720.
(19) El-Kaderi, H. M.; Hunt, J. R.; Mendoza-Cortes, J. L.; Cote, A. P.; Taylor, R. E.; O'Keeffe, M.; Yaghi, O. M. *Science* **2007**, *316*, 268–272.
(20) U.S. Department of Energy, Hydrogen, Fuel Cells and Infrastructure Technologies Multiyear Research, Development and Demonstration Plan, http://www1.eere.energy.gov/hydrogenandfuelcells/mypp/.
(21) Pei, J.; Ni, J.; Zhou, X.-H.; Cao, X.-Y.; Lai, Y.-H. *J. Org. Chem.* **2002**, *67*, 4924.
(22) Zimmermann, T. J.; Müller, T. J. J. *Synthesis* **2002**, *9*, 1157–1162.
(23) Aebischer, O. F.; Tondo, P.; Alameddine, B.; Jenny, T. A. *Synthesis* **2006**, *17*, 2891–2896.
(24) Latonen, R.-M.; Kvarnstrom, C.; Ivaska, A. *J. Electroanal. Chem.* **2001**, *512*, 36–48.
(25) Zhou, W.; Wu, H.; Hartman, M. R.; Yildirim, T. *J. Phys. Chem. C* **2007**, *111*, 16131–16137.
(26) Ma, S.; Eckert, J.; Forster, P.; Yoon, J.; Hwang, Y. K.; Chang, J.-S.; Collier, C. D.; Parise, J. B.; Zhou, H.-C. *J. Am. Chem. Soc.* **2008**, *130*, 15896–15902.
(27) Panella, B.; Hirscher, M.; Pütter, H.; Müller, U. *Adv. Funct. Mater.* **2006**, *16*, 520–524.
(28) Zapol, P. Private communication.

MA802394X